EUROPEAN ORGANIZATION FOR NUCLEAR RESEARCH

Letter of Intent to the ISOLDE and Neutron Time-of-Flight Committee

Exploring ^{14}O as an open quantum system with SpecMAT

May 12, 2021

B. Olaizola[1], Y. Ayyad[2,3], H. Álvarez[2], A. Arokia[4], M. Caamaño[2], J. Chen[5], A. Ceulemans[4], B. Fernández[2], S. Freeman[6], L. Gaffney[7], A. Illana[8], B. P. Kay[5], W. Mittig[3], A. Muñoz[2], R. Page[7], O. Poleshchuk[4], R. Raabe[4], D. Regueira-Castro[2], S. Wang[2], J.C Zamora[9]

[1]*ISOLDE-EP, CERN, CH-1211 Geneva 23, Switzerland*
[2]*IGFAE, Universidade de Santiago de Compostela, Santiago de Compostela, Spain*
[3]*Facility for Rare Isotope Beams, Michigan State University, East Lansing, MI, USA*
[4] *Instituut voor Kern-en Stralingsfysica, Katholieke Universiteit Leuven, Leuven, Belgium*
[5] *Physics Division, Argonne National Laboratory, Argonne, Illinois, USA*
[6] *Department of Physics and Astronomy, University of Manchester, Manchester, UK*
[7] *Department of Physics, University of Liverpool, Liverpool, UK*
[8] *University of Jyvaskyla, Department of Physics, University of Jyvaskyla, Finland*
[9] *Instituto de Fisica, Universidade de Sao Paulo, Sao Paulo, Brazil*

Spokesperson: [B. Olaizola] [bruno.olaizola@cern.ch]
Spokesperson: [Y. Ayyad] [yassid.ayyad@usc.es]
Contact person: [B. Olaizola] [bruno.olaizola@cern.ch]

CERN-INTC-2021-036 / INTC-I-231
12/05/2021

Abstract:

This letter of intent describes an experiment for the future SpecMAT+ISS. We aim to study excited levels in ^{14}O coupled to the continuum, where significant clustering effects can be expected. The resonances in ^{14}O will be populated in resonant scattering of ^{10}C on ^{4}He. The main physics goals are to extract information on the predicted linear-chain structures near the alpha emission threshold and investigate the competition between sequential and simultaneous two proton emission. Since SpecMAT has not been commissioned yet, we are sending this proposal as a Letter of Intent, which will be followed by a proposal once commissioning has been performed.

Requested shifts: No shifts requested at this stage
Installation: [2nd beamline (ISS + SpecMAT)]

1 Introduction

Well-bound nuclei can be considered as closed quantum systems that can be described by state-of-the-art versions of the shell model where nucleons occupy well localized single particle states. However, when we move towards the dripline or we excite the nucleus near threshold energies, the closed-system approximation stops being valid and the coupling to the continuum cannot be neglected any further. In these scenarios the nucleus behaviour is better described by that of a many-body open quantum system. This complex interplay between reaction and structure leads to intriguing phenomena where weakly bound or unbound systems exhibit features such as halos, superradiance, particle emission and alpha clustering. The latter is an ubiquitous phenomenon in low-energy nuclear physics that manifests all over the landscape revealing astonishing features of both, stable and radioactive nuclei. However, the origin and mechanism that explains the cluster formation is not yet fully understood [1]. There are two aspects that favor the formation of clusters: proximity to cluster emission threshold and deformation. Arguably, the most important clustering case is the so-called Hoyle state (0_2^+ at 7.65 MeV) in ^{12}C, a three alpha particle resonance that explains the formation of heavier elements in the universe.

When we move towards the neutron-rich region of the carbon isotopic chain, the shape of the states that exhibit a clusterized structure changes dramatically. Antisymmetrized molecular dynamics (AMD) calculations [2] suggest that the excess neutrons may stabilize the nucleus that forms molecular-like structures with the neutrons occupying bonding orbitals between the cluster cores. Such states appear near the alpha particle emission threshold, in general, featuring shapes where the alpha particles are arranged in triangular or linear fashion, among others (see the right band in Fig. 1). These effects have been studied for ^{14}C in several experiments, but the results did not yield unequivocal evidence of the existence of linear-chain states [3, 4, 5].

Given the isospin symmetry, it is logical to ask if valence protons could play also a glue-like role in binding alpha clusters just as neutrons probably do in ^{14}C. Therefore, it is most interesting to study the mirror symmetric ^{14}O to research how strong the charge symmetry is breaking in cluster states. Figure 1 shows AMD calculations [6] that predict linear chains in both members of the mirror pair ^{14}C-^{14}O. As can be seen, the charge symmetry breaking is predicted to be small for the first two calculated 0^+, and significantly larger for the third one. These same AMD calculations predict rotational bands on top of these 0^+ states, also suggesting that linear structure is rigid enough to not bend, at least up to the 4^+ states of their respective rotational bands. And even more interesting is the fact that the Thomas-Ehrman shift, the reduction of the Coulomb energy due to extended spatially extended s-wave levels, supports the existence of a σ-bond linear-chain state [6]. In addition, such states have a large decay width to the ^{10}C(2_1^+) and ^{10}Be(2_1^+) excited states, easily distinguishable by the kinematics of the reaction (see Ref. [4]). Therefore, this experiment aims at providing complementary proofs of the elusive linear-chain band in the ^{14}C-^{14}O.

Ref. [4] showed the capability of experiments using Active Target Time Projection Chambers (AT TPC) to identify rotational bands near cluster emission thresholds in ^{14}C using α scattering. The elastic scattering channel offers a wealth of information to identify the resonances in a wide energy-angle domain in center of mass (see Figure 2).

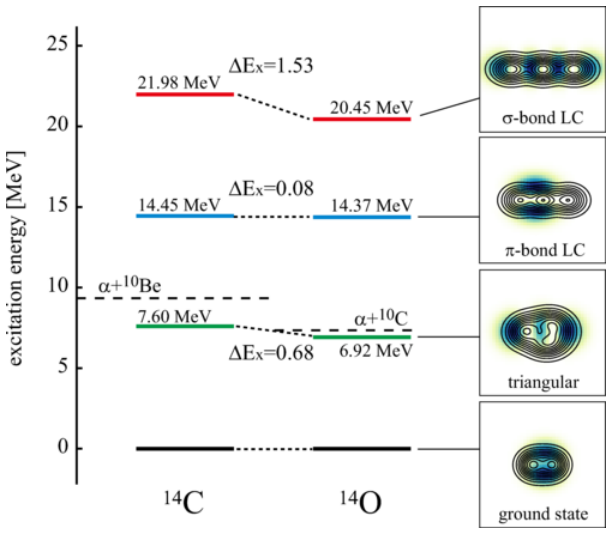

Figure 1: Figure taken from [6]. Theoretical AMD calculations of the α-cluster bandheads 0^+ states (colored lines) and the α emission thresholds (dashed lines) in the mirror nuclei ^{14}C and ^{14}O. ΔE_x indicates the energy difference between analog states. To the right, the different clustering shapes predicted for these states.

This is crucial to provide a reliable spin-parity assignment via R-matrix calculation since resonances with different angular momentum appear in different regions of the energy-angle matrix, as shown in the panel (a) of Fig. 2. Similarly, this experiment will use the SpecMAT and the ISS solenoid. Figure 3 shows the capability of such combination, yielding an increase energy resolution and particle identification.

Another example of near-threshold phenomena we expect to see in ^{14}O is two-proton emission ($2p$) [7, 8, 9]. The study of $2p$ is a powerful tool to understand three-body effects and clustering inside the nucleus. This emission can occur when a single or a pair of valence protons are above the strong nuclear potential well, but forms a resonant system with the core due to the Coulomb+centrifugal barrier. To be emitted, these proton must tunnel through said barrier, which height and width will determine its partial lifetime. This decay mode can proceed via three different competing mechanism: (i) three-body direct breakup, the so-called *democratic* decay, (ii) sequential emission of two protons via a state or resonance of an intermediate nucleus, and (iii) di-proton (^{2}He) cluster emission, in which the protons are emitted in a quasi-bound s configuration that breaks up after they tunnel trough the potential barrier. Decay mode (i) is considered a pure three-body breakup, while modes (ii) and (iii) can be interpreted as two consecutive two-body decays. More interestingly, whenever the $2p$ is energetically allowed ($Q_{2p} > 0$), there is a competition between the ^{2}He and sequential emissions, even when the $1p$ emission is energetically forbidden ($Q_{1p} < 0$) [10].

Most of the previous $2p$ studies were limited to the decay from the ground state [8, 9] or, in a few experiments, up to intermediate energies [12]. In such cases, the energy available in the decay and the resonance in the di-proton system present significant overlap and the separation is difficult. In this LoI, we propose to look at the competition between sequential and correlated two proton decay for ^{14}O with an emission energy well above

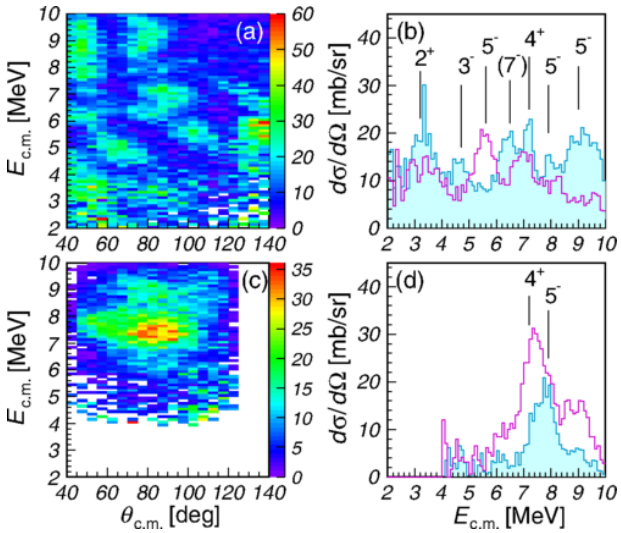

Figure 2: Differential cross sections of ^{10}Be scattering off α particles: (a) elastic scattering and (c) inelastic scattering to the 2_1^+ state of ^{10}Be. The color scale is given in mb/sr. Excitation functions for (b) elastic and (d) inelastic scattering also are shown. The shaded spectrum is gated by $\theta_{c.m.}$=70°–90°(45°–55°), and the blank spectrum by 90°–110°(70°–80°) for elastic (inelastic) scattering. The lines indicate identified resonances. Figure taken from [4].

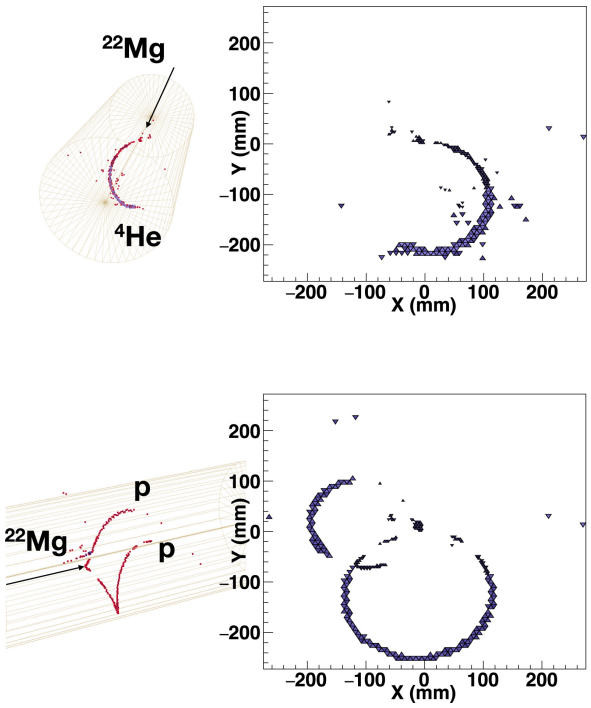

Figure 3: Upper panels: 3D hit pattern and projection into the pad plane of an ^{22}Mg(α,α) event. Lower panels: Same as the upper panels but for the ^{22}Mg$(\alpha,2p)$ channels. The particles can be easily distinguished because of the energy loss density along the trajectory. The traces were experimentally recorded using the AT-TPC inside a magnetic field at the ReA3 re-accelerator of the NSCL. Figure adapted from [11].

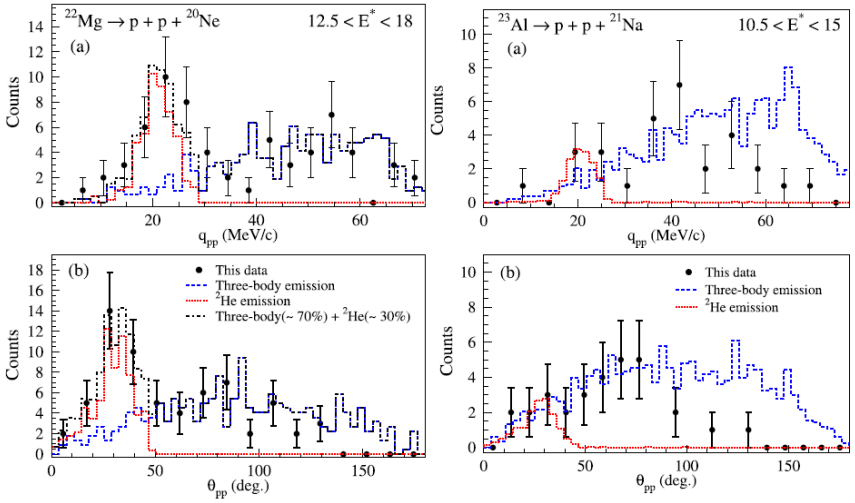

Figure 4: Figures taken from [12]. It shows the experimentally measured $2p$ emission for ^{22}Mg (*left*) and ^{23}Al (*right*). The two top plots marked (a) show the momentum distribution (q) of the protons and the two bottom ones, marked as (b) their angular distribution (θ). In the case of ^{22}Mg, there are clear peaks at q$\sim$ 20 MeV/c and $\theta \sim 30°$, a clear indication of a significant ^{2}He emission in the decay. In the case of ^{23}Al these features are not present, with very broad distribution both in angle and momentum, which was interpreted as pure three-body decay.

the $2p$ resonance as a function of the beam energy. At higher energies, an enhanced emission probability due to clustering and pairing may be expected, similar to the alpha cluster condensation predicted near to the $n-\alpha$ threshold. This is envisioned as a proof-of-principle, since such experiments have never been performed using a TPC. Shall the experiment succeed with the "easy-to-produce" ^{10}C beam, we plan on extending this kind of studies using more exotic nuclei closer to the proton dripline, where $2p$ emission should be greatly enhanced.

2 Relevant previous knowledge on ^{14}O

While there are levels in ^{14}O known up to $\sim$ 17 MeV, most of them do not have their decay mode reported [13], although they can be expected to have significant α emission branches once they are above the threshold at $\sim$ 10 MeV. Therefore, there is no experimental information on the possible α-clustering structure of this nucleus.

The 7.77-MeV state in ^{14}O was measured to have a strong $2p$ configuration outside the ^{12}C core in a $2p$-transfer reaction [14] and it is $\sim$ 1.2 MeV over the di-proton separation energy. The state was populated in a resonant proton scattering experiment using a fast ^{13}N beam observing a weak $2p$ branch [15]. By measuring the angular distribution between the two emitted protons, the authors claimed that the $2p$ decay mostly proceeds through a sequential manner via the $1/2^-_2$ state in ^{13}N.

A later experiment by Charity *et al* [16] expanded that work in a neutron knock-out reaction using a fast ^{15}O. In their work, the authors populated several states between

$\sim$ 7.7 and 11.2 MeV that presented $2p$ decay branches. For all populated states, they concluded that it was a sequential $2p$, with no significant ^{2}He emission or three-body break up.

3 Goals of the experiment

The main goal of the experiment is to study the ^{14}O nucleus as an open quantum system by its coupling to the continuum. We expect it to manifest mainly in two different clustering phenomena: molecular-like α-cluster linear chains and $2p$ emission. To do so we will employ SpecMAT [17] deployed in the magnetic field of the ISS solenoid. This will allow to study the whole energy range from the beam energy of 5 MeV/A down to the threshold energy Q thanks to the Active Target technique.

We expect to identify the three rotational bands near the α-emission threshold predicted by theory. The superior angular resolution of SpecMAT and its nearly 4π coverage with 100% efficiency will allow for a firm identification of the L of the different populated states. The results will be compared with existing state-of-the-art AMD calculations to elucidate the linear character of said bands.

The other phenomenon to be studied is the competition between direct and sequential $2p$ emission as a function of the beam energy, ^{10}C+^{4}He$\rightarrow^{14}$O* $\rightarrow^{12}$C+$2p$. The main difference with previous experiments is that the reaction ^{10}C+^{4}He$\rightarrow^{14}$O* has a large positive Q= +10.1 MeV. This way the reaction will populate states at significantly higher energies than previous similar experiments [15, 16]. This already presents an advantage, since for states from $\sim$ 11 MeV and higher there is virtually no information other than the energy [13].

The 3-body and sequential components will be disentangled following a similar method than work [12] (see Fig. 4). A pure 3-body decay is not expected to present any angular correlation or peak in the energy distribution. A two $1p$ sequential decay could present discrete energy peaks and a very subtle angular distribution. Lastly, the two protons of the ^{2}He emission should share the same energy due to momentum conservation and present a well define peak in the energy spectrum and similarly have a sharp angular distribution at low θ_{pp}. By recording the traces of the emitted particles, the experiment will be able to precisely measure their energies and angles of emission. Moreover, by running inside the strong magnetic field of ISS, this work will have a vast dynamic range and a superior energy and angular resolution than any previous experiment on $2p$ decay. This, in turn, will allow for a meaningful comparison to theoretical models that are currently being calculated [18].

In summary:

- **Extract the energy, spin-parity and width of resonances populated in resonant elastic and inelastic scattering of ^{10}C on ^{4}He.**
- **Identify the members of the predicted rotational linear-chain and triangular bands of ^{14}O through new clustering observables: Thomas-Erhman shifts, decay patterns to excited states and 3-body decay kinematics.**

- **Investigate the competition between sequential and simultaneous two proton emission on ^{14}O in a wide excitation energy range.**

4 Experimental details

Active Targets Time Projection Chambers are one of the best tools to perform this type of experiment [19, 20]. They provide high excitation energy resolution and luminosity, continuous measurement of the excitation function with a single beam energy, multiparticle emission reconstruction at very low energy and very forward angles in center of mass, and large dynamic range when used together with a solenoid magnet. Moreover, for particular experiment, they enable the measurement of almost every reaction channel with high efficiency thanks to the high efficiency and the trigger scheme.

The experiment will be performed using SpecMAT [17] filled with a pure ^{4}He gas at 1 bar and placed inside ISS magnetic field of 2.5 T. The gas will serve both, as a target for the reaction and as a tracking medium for the emitted particles. The length of the detector (30 cm) corresponds to a thickness of around 8×10^{20} ^{4}He/cm^2. The electrons produced this way will be guided by an applied homogeneous electric field and collected on a highly-pixelated pad plane. A 2D reconstruction can be directly extracted from the fired pads, and the 3D on the electron drift time in the gas. These 3-dimensional tracks contain information about the particle, its energy and lab-angle. The ISS magnetic field parallel to the beam path will bend the trajectories of charged particles emitted in the reaction, providing an additional identification by measuring their magnetic rigidity.

The pressure of the gas is chosen to investigate the region of interest of resonances in ^{14}O. With a 5A MeV ^{10}C beam, we cover from 26 MeV down to 20 MeV of excitation energy (taking into account Q=-10.12 MeV). This region covers the 0^+, 2^+ and the 4^+ members of the σ-bond band of the linear-chain (see Fig. 1). This is the band where the effects of the Coulomb displacement are more evident, as predicted by AMD calculations [6]. For the determination of π-bond band and part of the triangular band (2^+ and the 4^+) the beam energy will be reduced to 3A MeV. Two proton emission is expected to appear within both energy domains. All this information never deduced before will allow us to perform a comprehensive study of the open quantum system nature of ^{14}O.

Due to the large decay width of α-clustering resonances, the cross sections are relatively large, $\sigma \sim 10$ mb/sr with a width of the resonance of about 500 keV. These large σ and the thickness of the detector are important to perform the experiment with a comfortable beam intensity and operate the detector under stable conditions. The dominant reaction channel, elastic scattering, is also the most important in this experiment. A beam intensity of around 10^4 pps should suffice to obtain few hundred counts per 10^o angular bin and per 100 keV (in center of mass) for the π-bond and triangular configurations in a few days. This corresponds to an instantaneous rate of about 10^5, adequate for SpecMAT as it features a hole in the pad plane where the unreacted beam passes through.

While not crucial to the experiment, the $CeBr_3$ ancillary array can be employed to identify decays into excited states of ^{10}C (fingerprint of the linear-chain band), levels populated in the proton emission and a possible competition between charged particle emission and gamma decay from this levels.

References

[1] Jacek Okołowicz, Marek Płoszajczak, and Witold Nazarewicz. On the Origin of Nuclear Clustering. *Progress of Theoretical Physics Supplement*, 196:230–243, 10 2012.

[2] Tadahiro Suhara and Yoshiko Kanada-En'yo. Cluster structures of excited states in ^{14}C. *Phys. Rev. C*, 82:044301, Oct 2010.

[3] M. Freer, J. D. Malcolm, N. L. Achouri, N. I. Ashwood, D. W. Bardayan, S. M. Brown, W. N. Catford, K. A. Chipps, J. Cizewski, N. Curtis, K. L. Jones, T. Munoz-Britton, S. D. Pain, N. Soić, C. Wheldon, G. L. Wilson, and V. A. Ziman. Resonances in 14C observed in the 4He(10Be,α)10Be reaction. *Physical Review C*, 90(5):054324, nov 2014.

[4] A. Fritsch, S. Beceiro-Novo, D. Suzuki, W. Mittig, J. J. Kolata, T. Ahn, D. Bazin, F. D. Becchetti, B. Bucher, Z. Chajecki, X. Fang, M. Febbraro, A. M. Howard, Y. Kanada-En'yo, W. G. Lynch, A. J. Mitchell, M. Ojaruega, A. M. Rogers, A. Shore, T. Suhara, X. D. Tang, R. Torres-Isea, and H. Wang. One-dimensionality in atomic nuclei: A candidate for linear-chain α clustering in C 14. *Physical Review C*, 93(1):014321, jan 2016.

[5] H. Yamaguchi, D. Kahl, S. Hayakawa, Y. Sakaguchi, K. Abe, T. Nakao, T. Suhara, N. Iwasa, A. Kim, D. H. Kim, S. M. Cha, M. S. Kwag, J. H. Lee, E. J. Lee, K. Y. Chae, Y. Wakabayashi, N. Imai, N. Kitamura, P. Lee, J. Y. Moon, K. B. Lee, C. Akers, H. S. Jung, N. N. Duy, L. H. Khiem, and C. S. Lee. Experimental investigation of a linear-chain structure in the nucleus14C. *Physics Letters, Section B: Nuclear, Elementary Particle and High-Energy Physics*, 766:11–16, 2017.

[6] T. Baba and M. Kimura. Coulomb shift in the mirror pair of ^{14}C and ^{14}O as a signature of the linear-chain structure. *Phys. Rev. C*, 99:021303, Feb 2019.

[7] V.I. Goldansky. On neutron-deficient isotopes of light nuclei and the phenomena of proton and two-proton radioactivity. *Nuclear Physics*, 19:482–495, 1960.

[8] J. Giovinazzo, B. Blank, M. Chartier, S. Czajkowski, A. Fleury, M. J. Lopez Jimenez, M. S. Pravikoff, J.-C. Thomas, F. de Oliveira Santos, M. Lewitowicz, V. Maslov, M. Stanoiu, R. Grzywacz, M. Pfützner, C. Borcea, and B. A. Brown. Two-proton radioactivity of ^{45}Fe. *Phys. Rev. Lett.*, 89:102501, Aug 2002.

[9] M. Pfützner, E. Badura, C. Bingham, B. Blank, M. Chartier, H. Geissel, J. Giovinazzo, L.V. Grigorenko, R. Grzywacz, M. Hellström, Z. Janas, J. Kurcewicz, A.S. Lalleman, C. Mazzocchi, I. Mukha, G. Münzenberg, C. Plettner, E. Roeckl, K.P. Rykaczewski, K. Schmidt, R.S. Simon, M. Stanoiu, and J.-C. Thomas. First evidence for the two-proton decay of ^{45}Fe. *The European Physical Journal A*, 14:279, 2002.

[10] Bertram Blank and Marek Płoszajczak. Two-proton radioactivity. *Reports on Progress in Physics*, 71(4):046301, mar 2008.

[11] Y. Ayyad, N. Abgrall, T. Ahn, H. Álvarez Pol, D. Bazin, S. Beceiro-Novo, L. Carpenter, R.J. Cooper, M. Cortesi, A.O. Macchiavelli, W. Mittig, B. Olaizola, J.S. Randhawa, C. Santamaria, N. Watwood, J.C. Zamora, and R.G.T. Zegers. Next-generation experiments with the active target time projection chamber (at-tpc). *Nuclear Instruments and Methods in Physics Research Section A: Accelerators, Spectrometers, Detectors and Associated Equipment*, 954:161341, 2020. Symposium on Radiation Measurements and Applications XVII.

[12] Y.G. Ma, D.Q. Fang, X.Y. Sun, P. Zhou, Y. Togano, N. Aoi, H. Baba, X.Z. Cai, X.G. Cao, J.G. Chen, Y. Fu, W. Guo, Y. Hara, T. Honda, Z.G. Hu, K. Ieki, Y. Ishibashi, Y. Ito, N. Iwasa, S. Kanno, T. Kawabata, H. Kimura, Y. Kondo, K. Kurita, M. Kurokawa, T. Moriguchi, H. Murakami, H. Ooishi, K. Okada, S. Ota, A. Ozawa, H. Sakurai, S. Shimoura, R. Shioda, E. Takeshita, S. Takeuchi, W.D. Tian, H.W. Wang, J.S. Wang, M. Wang, K. Yamada, Y. Yamada, Y. Yasuda, K. Yoneda, G.Q. Zhang, and T. Motobayashi. Different mechanism of two-proton emission from proton-rich nuclei 23al and 22mg. *Physics Letters B*, 743:306–309, 2015.

[13] F. Ajzenberg-Selove. Energy levels of light nuclei a = 13–15. *Nuclear Physics A*, 523(1):1–196, 1991.

[14] M. B. Greenfield, C. R. Bingham, E. Newman, and M. J. Saltmarsh. (^{3}He, n) reaction at 25 mev. *Phys. Rev. C*, 6:1756–1769, Nov 1972.

[15] C.R. Bain, P.J. Woods, R. Coszach, T. Davinson, P. Decrock, M. Gaelens, W. Galster, M. Huyse, R.J. Irvine, P. Leleux, E. Lienard, M. Loiselet, C. Michotte, R. Neal, A. Ninane, G. Ryckewaert, A.C. Shotter, G. Vancraeynest, J. Vervier, and J. Wauters. Two proton emission induced via a resonance reaction. *Physics Letters B*, 373(1):35–39, 1996.

[16] R. J. Charity, K. W. Brown, J. Okołowicz, M. Płoszajczak, J. M. Elson, W. Reviol, L. G. Sobotka, W. W. Buhro, Z. Chajecki, W. G. Lynch, J. Manfredi, R. Shane, R. H. Showalter, M. B. Tsang, D. Weisshaar, J. R. Winkelbauer, S. Bedoor, and A. H. Wuosmaa. Invariant-mass spectroscopy of ^{14}O excited states. *Phys. Rev. C*, 100:064305, Dec 2019.

[17] Riccardo Raabe. The SpecMAT active target. Technical report, CERN, Geneva, Jan 2020.

[18] S. M. Wang and W. Nazarewicz. Fermion pair dynamics in open quantum systems. *Phys. Rev. Lett.*, 126:142501, Apr 2021.

[19] D. Bazin, T. Ahn, Y. Ayyad, S. Beceiro-Novo, A.O. Macchiavelli, W. Mittig, and J.S. Randhawa. Low energy nuclear physics with active targets and time projection chambers. *Progress in Particle and Nuclear Physics*, 114:103790, 2020.

[20] Ayyad, Y., Bazin, D., Beceiro-Novo, S., Cortesi, M., and Mittig, W. Physics and technology of time projection chambers as active targets. *Eur. Phys. J. A*, 54(10):181, 2018.

Appendix

DESCRIPTION OF THE PROPOSED EXPERIMENT

The experimental setup comprises: (*name the fixed-ISOLDE installations, as well as flexible elements of the experiment*)

Part of the	Availability	Design and manufacturing
ISS + SpecMat	☒ Existing	☒ To be used without any modification
[Part 1 of experiment/ equipment]	☐ Existing	☐ To be used without any modification ☐ To be modified
	☐ New	☐ Standard equipment supplied by a manufacturer ☐ CERN/collaboration responsible for the design and/or manufacturing
[Part 2 of experiment/ equipment]	☐ Existing	☐ To be used without any modification ☐ To be modified
	☐ New	☐ Standard equipment supplied by a manufacturer ☐ CERN/collaboration responsible for the design and/or manufacturing
[insert lines if needed]		

HAZARDS GENERATED BY THE EXPERIMENT (if using fixed installation:) Hazards named in the document relevant for the fixed [MINIBALL + only CD, MINIBALL + T-REX] installation.

Additional hazards:

Hazards	[Part 1 of experiment/ equipment]	[Part 2 of experiment/ equipment]	[Part 3 of experiment/ equipment]
Thermodynamic and fluidic			
Pressure	[pressure][Bar], [volume][l]		
Vacuum			
Temperature	[temperature] [K]		
Heat transfer			
Thermal properties of materials			
Cryogenic fluid	[fluid], [pressure][Bar], [volume][l]		
Electrical and electromagnetic			
Electricity	[voltage] [V], [current][A]		
Static electricity			
Magnetic field	[magnetic field] [T]		
Batteries	☐		

Capacitors	□		
Ionizing radiation			
Target material [material]			
Beam particle type (e, p, ions, etc)			
Beam intensity			
Beam energy			
Cooling liquids	[liquid]		
Gases	[gas]		
Calibration sources:	□		
• Open source	□		
• Sealed source	□ [ISO standard]		
• Isotope			
• Activity			
Use of activated material:			
• Description	□		
• Dose rate on contact and in 10 cm distance	[dose][mSV]		
• Isotope			
• Activity			
Non-ionizing radiation			
Laser			
UV light			
Microwaves (300MHz-30 GHz)			
Radiofrequency (1-300 MHz)			
Chemical			
Toxic	[chemical agent], [quantity]		
Harmful	[chem. agent], [quant.]		
CMR (carcinogens, mutagens and substances toxic to reproduction)	[chem. agent], [quant.]		
Corrosive	[chem. agent], [quant.]		
Irritant	[chem. agent], [quant.]		
Flammable	[chem. agent], [quant.]		
Oxidizing	[chem. agent], [quant.]		
Explosiveness	[chem. agent], [quant.]		
Asphyxiant	[chem. agent], [quant.]		
Dangerous for the environment	[chem. agent], [quant.]		
Mechanical			

Physical impact or mechanical energy (moving parts)	[location]		
Mechanical properties (Sharp, rough, slippery)	[location]		
Vibration	[location]		
Vehicles and Means of Transport	[location]		
Noise			
Frequency	[frequency],[Hz]		
Intensity			
Physical			
Confined spaces	[location]		
High workplaces	[location]		
Access to high workplaces	[location]		
Obstructions in passageways	[location]		
Manual handling	[location]		
Poor ergonomics	[location]		

Hazard identification:

Average electrical power requirements (excluding fixed ISOLDE-installation mentioned above): [make a rough estimate of the total power consumption of the additional equipment used in the experiment]: ... kW